

# Design of Dual Polarised Wide Band Plane Wave Generator for Direct Far-Field Testing

F. Scattone<sup>1</sup>, D. Sekuljica<sup>1</sup>, A. Giacomini<sup>1</sup>, F. Saccardi<sup>1</sup>,  
 A. Scannavini<sup>2</sup>, N. Gross<sup>2</sup>, E. Kaverine<sup>2</sup>, P. O. Iversen<sup>2</sup>, L. J. Foged<sup>1</sup>  
<sup>1</sup> MVG, Microwave Vision Italy SRL, Pomezia, Italy, lars.foged@mvg-world.com  
<sup>2</sup> MVG, Microwave Vision HQ, Paris, France, peri@orbitfr.com

**Abstract**— The Plane Wave Generator (PWG) is intended to generate a local plane wave in its close proximity. It consists of an array of elements with optimized complex excitation and disposed on a suitable lattice. The PWG achieves far-field testing condition in a spherical Quiet Zone (QZ) where the antenna under test (AUT) can be directly measured. The testing method is similar to a Compact Antenna Test Range (CATR), but a considerably smaller space is required.

Early PWG designs have been limited to narrow-band and single polarization. In this paper we present the design and measured performance of a dual-polarized PWG with 10:1 bandwidth. The prototype has been tested in the 0.6-6 GHz frequency range. In the following, we show the initial testing results on the QZ uniformity and an initial evaluation of the achievable measurement accuracy.

**Index Terms**—antenna, measurement, phased array

## I. INTRODUCTION

The Plane Wave Generator (PWG) is a flexible indoor antenna testing system for the direct measurement of the far-field performance [1]. It allows the measurement of the complete spherical radiation pattern of antenna under test (AUT), through the mechanical rotation of the AUT (or the PWG itself) in the 3D space. The PWG system shares many characteristics of the modern Compact Antenna Test Ranges (CATRs). The main advantage of the PWG consists of a smaller physical size, requiring a considerably smaller anechoic chamber. This feature becomes more important as the frequency decreases. This is the case of the sub-6 GHz band, typical of 4G and upcoming 5G applications. Furthermore, the uncertainty contributions to the measurement accuracy are similar to the CATR, removing the contribution of the direct illumination of the Quiet Zone (QZ) by the reflector feed.

The PWG implementations proposed in literature are limited to theoretical designs or to narrow band prototypes with single polarization [2-7]. To optimize the measurement equipment, the costs and the acquisition time, a PWG should be wideband and dual-polarized. In this paper we present the design of our dual-polarized PWG demonstrator working in a 10:1 band, from 600 MHz to 6 GHz.

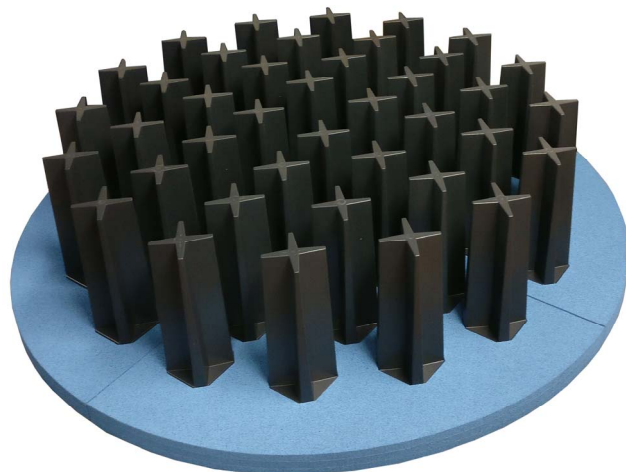


Fig. 1. PWG prototype. It consist of 40 dual polarized, wide bandwidth elements disposed on four circular lattices. The elements are mounted on an absorber covered metallic ground-plane.

## II. SYSTEM DESIGN

The PWG system can be divided in three main blocks: the beam forming network (BFN), the antenna array and the radiating element.

The BFN is needed to weight the complex excitation coefficients of the array elements. A passive BFN using attenuator and phase shifters is the simplest implementation to reach this goal. However, this solution is not effective when a wide bandwidth is required, since the excitation coefficients of the array are strongly frequency dependent. On the other end of the spectrum, a fully digital BFN would fulfill a wideband requirement, providing additional degrees of freedom to the system. Unfortunately, increasing the size of the array and the number of radiating elements, this solution becomes unfeasible or extremely costly. A practical cost-effective solution can be found halfway among the two cited above: the array can be divided in sub-arrays while a reduced number of parallel transceivers modules controls the complex excitation of the sub-arrays. This method allows the frequency dependent excitation and the wide bandwidth, lowering down the number of active controls.

### III. ARRAY DESIGN

A circular array of concentric rings of elements is considered, as the most natural way to generate a spherical QZ. Each ring represents a sub-array, where all the elements are excited with the same complex excitation. The design rules for the array have been presented in [2, 3]. The procedure is based on the optimal sampling theory [4, 5].

The design of the array element comes from a trade-off between bandwidth, physical dimension and directivity. The bandwidth must be sufficiently large to support the capabilities of the system. The physical dimension must be sufficiently small to fit the element in the array lattice, but large enough to have an average directivity. A high directivity helps to reduce the mutual coupling between the elements, while a low directivity is more suitable to illuminate a QZ. Also, dual-polarization is required.

### IV. ARRAY EXCITATION SYNTHESIS

The synthesis domain is represented by a discrete number of points defining the QZ, where the radiated field is determined, using a representative numerical model or by post-processing the measurements of the array element. The excitation synthesis is performed through a non-linear optimization, minimizing an objective function. In this case, the objective function is not limited to the minimization of the maximum deviation of the field in the QZ, but also optimizes the total energy falling in the QZ. The advantage of this formulation is to avoid unwanted field outside the synthesis domain, also alleviating the required efficiency of the anechoic chamber absorbers.

### V. PWG PROTOTYPE

A prototype of the PWG in the frequency range 0.6-6 GHz has been manufactured and tested. The goal is to synthesize a spherical QZ with a diameter of 480 mm centered at a distance of 950 mm from the array aperture.

The resulting PWG is a four-ring array, with a total of 40 elements and an overall diameter of 800 mm, including the surrounding absorber. Each ring represents a sub-array with a different excitation coefficient. All the elements of a ring share the same excitation. The BFN is formed by simple power dividers and phase matched cables, equally distributing the power among the elements of the ring with the least phase mismatch.

The array element must be an ultra-wide band dual-polarized antenna covering the 0.6 GHz-6 GHz, fitting the array lattice. Such element has been designed and integrated in the PWG prototype, as shown in Fig. 1. Here, the 40 elements are mounted on a metallic ground plane. The latter has been covered with MVG AEL absorbers, embedding the array elements and reducing mutual coupling and spurious waves.

### VI. MEASURED QUIET ZONE PERFORMANCE

The PWG prototype has been measured in the MVG StarGate 64 as shown in Fig. 2.

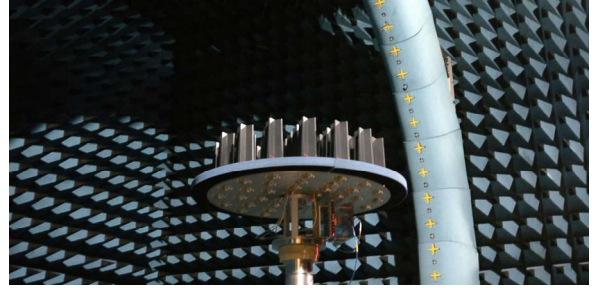


Fig. 2. PWG during validation measurement in the spherical NF multi probe system SG-64

The measurement has been performed separately of each of the four rings. The radiated field of each ring has been evaluated on the 3-dimensional space of the QZ, using post-processing techniques. The fields have been, then, combined with the suitable excitation coefficients as explained in Sec. IV. The measured performance of the PWG in terms of amplitude and phase variation with respect to an ideal plane wave on the resulting QZ with optimum excitation are shown in Fig. 3 and Fig. 4, respectively.

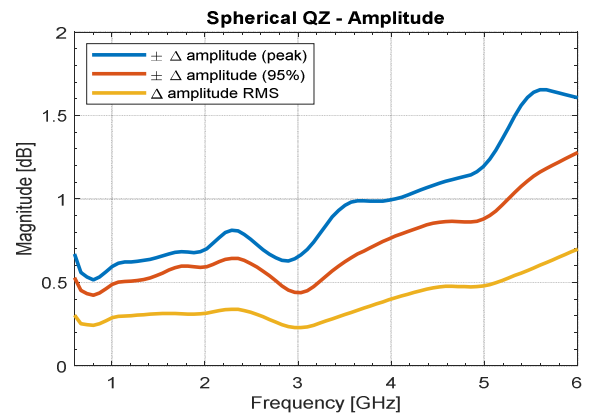


Fig. 3. Amplitude variation in spherical QZ of diameter 480 mm 950 mm from the PWG aperture.

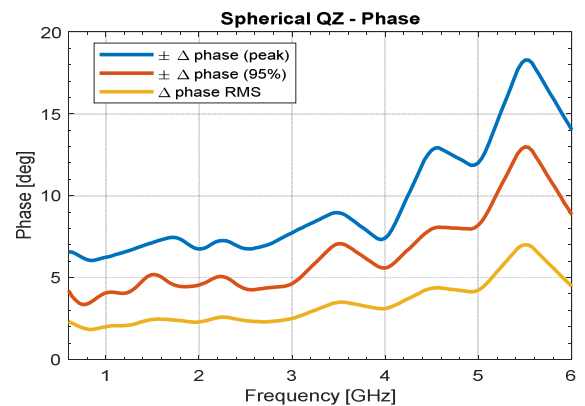


Fig. 4. Phase variation in spherical QZ of diameter 480 mm at 950 mm from the PWG aperture.

The results refer to the radiated field in the spherical volume of the QZ with diameter 480 mm centered at 950 mm from the aperture. The reported values of amplitude and phase variation within the entire QZ volume are extremely low at frequencies up to 4 GHz and increase in the higher part of the band, still maintaining the variation with acceptable levels. The values of the 95% percentile and the RMS variation are also strong indicators that the variation on the QZ volume from the ideal plane wave is within acceptable limits.

The quality of the QZ can also be examined by inspecting a plan cut of the radiated field on a plane parallel to the aperture, containing the center of the QZ sphere. Fig. 5 shows such a cut in amplitude. The phase of the field on the same plane is shown in Fig. 6.

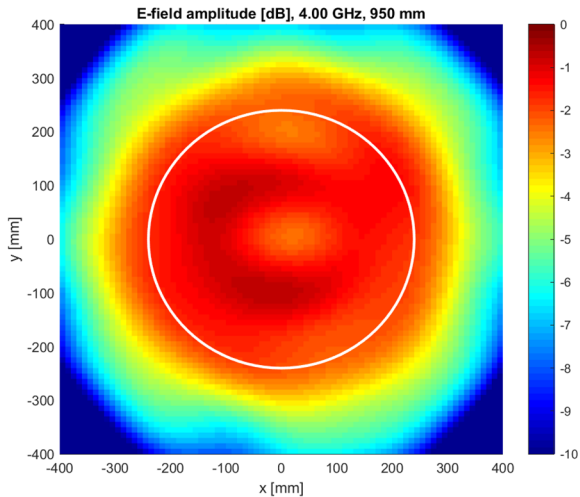


Fig. 5. E-field amplitude map of QZ center @ 4 GHz. The white ring shows the QZ dimension.

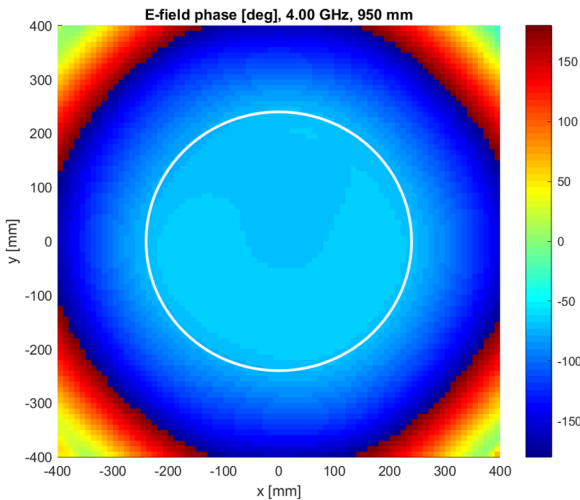


Fig. 6. E-field phase map of QZ center @ 4 GHz. The white ring shows the QZ dimension.

In Fig. 7, the field amplitude on the QZ in the plane orthogonal to the array aperture, is shown at 4 GHz. This image is a down-range field map containing the propagation direction and shows the homogeneity of the QZ field.

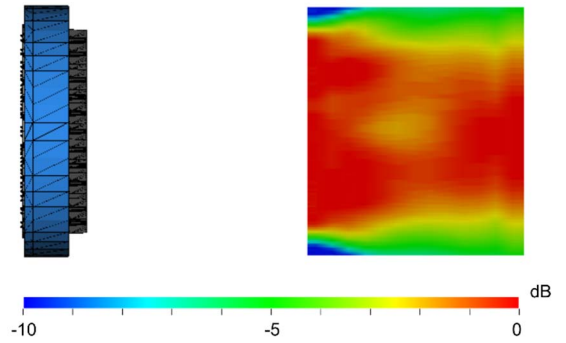


Fig. 7. E-field amplitude map in the QZ area @ 4 GHz along the direction of propagation.

## VII. EMULATION OF MEASUREMENT WITH PWG

To test the performance of the PWG prototype in the measurement of an AUT, we emulated different measurement scenarios using the transmission formula [8]. The formula can be used to emulate the coupling between a transmitting antenna (the AUT) and a receiving device (such as the PWG), knowing the spherical wave spectrum of both. In particular, we considered two different AUTs: a standard gain horn (SGH) and the MVG SH2000 horn antenna [9]. The considered SGH has an aperture of 450 mm x 337.5 mm, slightly larger than the QZ, with a directivity close to 22 dBi at 4 GHz. The SGH is shown in the left part of Fig. 8, with the QZ represented by an orange sphere. The SH2000 is a smaller dual-ridge horn antenna with dimensions 105 mm x 61 mm. For the measurement emulation, the antenna is placed off-set on the edge of the QZ. The measurement setup is represented in the right part of Fig. 8.

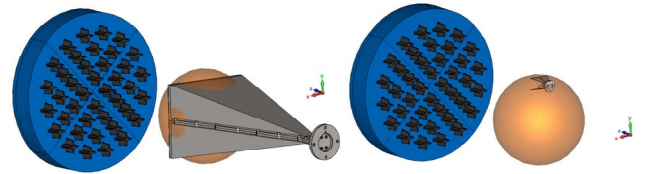


Fig. 8. Left: measurement setup with onset SGH. The antenna is slightly larger than the QZ (in orange). Right: measurement setup with offset SH2000. The antenna is placed in the top edge of the QZ.

The measurement with the PWG is compared to the results of a second emulation, using single element of the array as measurement antenna. In both cases, PWG and single antenna, the measurement distance is 950 mm and the far-field condition is not reached.

The SGH and SH2000 directivity patterns are shown in Fig. 9, respectively at the top and the bottom. In both cases, we show the reference pattern (green), the measurement with the PWG (cyan) and the one with the single element (magenta) at 4 GHz. In the case of the SGH, the single element reproduces a strongly distorted pattern with a 4 dBi directivity reduction. Also for the SH2000, the radiation pattern obtained with the single element is altered, with a 12° deviation from the boresight. Conversely, the PWG is able to generate a high-

fidelity radiation patterns for the SGH and the off-set SH2000, with accurate directivity levels, side lobe levels and nulls.

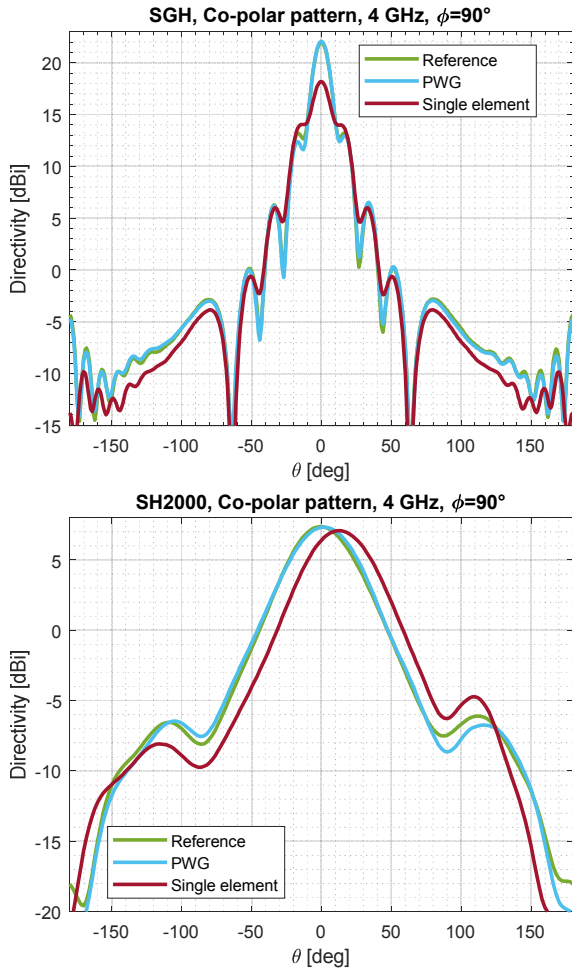


Fig. 9. E-plane radiation pattern of the SGH (top) and SH2000 (bottom). Both sub-figures show the comparison between the reference pattern (green), the emulated measurement with the PWG (cyan) and with the single element (magenta).

The Equivalent Error Level (ENL) [10] can be used to evaluate the accuracy of the measurement. The ENL is defined as:

$$ENL = 20 \log_{10} \left( RMSE \left| \frac{E(\theta, \varphi) - \tilde{E}(\theta, \varphi)}{E(\theta, \varphi)_{MAX}} \right| \right) \quad (1)$$

where  $E(\theta, \varphi)$  is the reference pattern and  $\tilde{E}(\theta, \varphi)$  is the test pattern. The co-polar and cross-polar ENL achieved in each emulated measurement is summarized in Table I together with the boresight directivity error.

TABLE I. MEASUREMENT ACCURACY

AUT	Receiving Device	Directivity Error (dB)	ENLco (dB)	ENLex (dB)
SGH	Single Element	+3.8	-23.7	-48.0
SGH	PWG	-0.1	-45.4	-51.6
Offset SH2000	Single Element	+1.0	-21.1	-26.8
Offset SH2000	PWG	0.0	-35.4	-38.8

## VIII. CONCLUSION

The concepts of an ultra-wide band, dual polarized Plane Wave Generator (PWG) has been presented in this paper. A prototype has been designed, manufactured and measured in the 600 MHz to 6 GHz frequency band. Performance indicators in terms of amplitude and phase uniformity of the generated QZ has been presented and the results are encouraging. The measured PWG has been used to emulate a measurement in two challenging cases, showing excellent performance.

The development of the PWG is an ongoing project. Further results will be presented during the conference.

## REFERENCES

- [1] "IEEE Standard Test Procedures for Antennas," *ANSI/IEEE Std 149-1979*.
- [2] A. Buonanno, M. D'Urso, and G. Prisco, "Reducing Complexity in Indoor Array Testing," *IEEE Transactions on Antennas and Propagation*, vol. 58, no. 8, pp. 2781-2784, Aug. 2010.
- [3] O. M. Bucci, M. D. Migliore, G. Panariello, and D. Pinchera, "Plane-Wave Generators: Design Guidelines, Achievable Performances and Effective Synthesis," *IEEE Transactions on Antennas and Propagation*, vol. 61, no. 4, pp. 2005-2018, Apr. 2013.
- [4] O. M. Bucci, C. Gennarelli, and C. Savarese, "Fast and accurate near-field-far-field transformation by sampling interpolation of plane-polar measurements," *IEEE Transactions on Antennas and Propagation*, vol. 39, no. 1, pp. 48-55, Jan. 1991.
- [5] O. M. Bucci, C. Gennarelli, and C. Savarese, "Representation of electromagnetic fields over arbitrary surfaces by a finite and nonredundant number of samples," *IEEE Transactions on Antennas and Propagation*, vol. 46, no. 3, pp. 351-359, Mar. 1998.
- [6] A. Capozzoli, C. Curcio, G. D'Elia, A. De Simone, A. Liseno, "An optimized approach to plane wave synthesis", Proc. of the *29th Annual Antenna Measur. Tech. Ass. Symp.*, 2008.
- [7] A Capozzoli, C Curcio, G D'elia, A Liseno, G Ianniello, and P Vinetti, "Effective 2D generalised plane wave synthesizers: Experimental validation", Proc. of the *30th Annual Antenna Measur. Tech. Ass. Symp.*, 2009.
- [8] J. E. Hansen (ed.), "Spherical Near-Field Antenna Measurements", *Peter Peregrinus Ltd.*, London, United Kingdom, 1988
- [9] [https://www.mvg-world.com/en/system/files/dual-ridge\\_horns\\_11\\_17.pdf](https://www.mvg-world.com/en/system/files/dual-ridge_horns_11_17.pdf)
- [10] M. A. Saporetti et al., "Measurements and simulations correlation of high reliability reflector antenna," Proc of the *10th European Conference on Antennas and Propagation (EuCAP)*, 2016.